



Concept, modeling and experimental evaluation of an integrated cooling, heating and thermoelectric generation system

Fernando Neves Quintino dos Santos¹ · Alex Roger Almeida Colmanetti¹ · Luben Cabezas-Gómez¹ · Cristiano Bigonha Tibiriçá¹

Received: 18 April 2022 / Accepted: 11 September 2022 / Published online: 25 September 2022
© The Author(s), under exclusive licence to The Brazilian Society of Mechanical Sciences and Engineering 2022

Abstract

A concept of an integrated system for cooling, heating and electricity generation using thermoelectric effect and water is presented. The concept consists of two 2-L capacity water reservoirs: The first one has been used to store cold water and the second one to store heated water. Both reservoirs are thermally connected by two thermoelectric modules, which can be used to heat and cool the water when supplying electrical energy to the modules or generate electricity when hot and cold water are stored in these two reservoirs. A theoretical model of the system is developed for transient simulation where heat transfer and energy conservation differential equations were numerically solved and a real prototype was built. The model uses the maximum performance parameters available in commercial thermoelectric datasheets to obtain all other relevant thermoelectric variables. The agreement between the developed model and the experiment was close to 95%, and the proposed system was able to cool water near zero degrees Celsius, to heat it near the water boiling point, and generate more than 1.5 W of electrical power when operated as thermoelectric generator using heated water and cold water with 70 °C temperature. The simulations also showed that water reservoirs of 25 L capacity, with initial temperatures of 95 °C for hot water and 25 °C for cold water, can be used to supply peak electrical power of 2.3 W and mean power of 1 W for 12 h, energy equivalent 6 AA alkaline batteries. This system has the potential to be applied for sustainable cooling, heating and electricity generation in isolated communities and in non-urban regions.

Keywords Cooling · Heating · Peltier effect · Power generation · Thermoelectric effect

List of symbols

A_{peltier}	Area of the Peltier module (specified by manufacturer)	m_C	Equivalent inertia of the cold reservoir
$c_{p,C}$	Specific heat of the water on the cold reservoir	m_H	Equivalent inertia of the hot reservoir
$c_{p,H}$	Specific heat of the water on the hot reservoir	Q_C	Heat transfer to the cold reservoir
COP_C	Coefficient of performance for cooling	Q_H	Heat transfer from the cold reservoir
COP_H	Coefficient of performance for heating	Q_{in}	Heat transfer entering the control volume
i	Electric current	Q_{max}	Maximum heat transfer of the module (specified by manufacturer)
i_{max}	Module input current causing maximum temperature difference	Q_{out}	Heat transfer exiting the control volume
k	Thermal conductivity	R_{cer}	Thermal resistance of the ceramic electric insulation layer
K_m	Module thermal conductance	R_{CR}	Contact thermal resistance
		$R_{\text{cond,TI}}$	Conduction thermal resistance of the thermal insulation
		$R_{\text{conv,air}}$	Natural convection thermal resistance of the air
		$R_{\text{conv,wat}}$	Natural convection thermal resistance of the water
		R_{CR}	Contact thermal resistance
		$R_{\text{env,C}}$	Thermal resistance between the environment and water in the cold reservoir

Technical Editor: Ahmad Arabkoohsar.

✉ Cristiano Bigonha Tibiriçá
bigonha@sc.usp.br

¹ Heat Transfer Research Group, Department of Mechanical Engineering, São Carlos School of Engineering, University of São Paulo, São Carlos, Brazil

$R_{env,H}$	Thermal resistance between the environment and water in the hot reservoir
R_{HS}	Heat sink thermal resistance
R_L	Electrical resistance of the load to which the generator is connected
R_m	Electrical resistance of the module
R_{rad}	External radiation thermal resistance
$R_{th,m}$	Thermal resistance between the cold and hot junctions of the module
$R_{thm,C}$	Thermal resistance between the module and the cold reservoir
$R_{thm,H}$	Thermal resistance between the module and the hot reservoir
S	Seebeck coefficient
S_m	Seebeck coefficient of the module
T_C	Water temperature in the cold reservoir
$T_{C,m}$	Module cold junction temperature
T_{env}	Environment temperature
T_H	Water temperature in the hot reservoir
$T_{H,m}$	Module hot junction temperature
$T_{H,ref}$	Module hot junction temperature reference
V_{thm}	Maximum voltage on the module (specified by manufacturer)
V_{thm}	Electric voltage on the module
W_{ele}	Electrical power
Z_m	Figure of merit of the module
ZT	Dimensionless figure of merit
ZT_m	Dimensionless figure of merit of the thermoelectric module
ΔT_{max}	Maximum temperature difference within the module (specified by manufacturer)
ΔT_{thm}	Temperature difference between the pair within the module
η	Efficiency of the thermoelectric generator
σ	Electrical conductivity

1 Introduction

Sustainable development and reduction of carbon emissions are a global concerns [1, 2]. New technologies and advances are being developed, notably highly efficient low fluid charge heat exchangers based on microchannels [3], low GWP alternatives [4] and photovoltaic generation [5, 6]. In this context, thermoelectric devices are an interesting alternative, as they can cool/heat or generate power, with no direct emissions.

Thermoelectricity is the phenomenon of converting thermal energy into electrical energy or vice versa that occurs when two electrical conductors made of different materials are combined, resulting in a thermoelectric pair [7, 8]. This phenomenon is related to the complementary Seebeck and Peltier effects, defined, respectively, as the conversion of

thermal to electrical energy when a temperature gradient is imposed, or the conversion of electrical to thermal energy when an electrical potential difference is applied on the thermoelectric pair. The Thomson effect is also present and it is related to the heat flow associated with the temperature gradient and electrical current flowing in a conductor. The Joule heating also occurs in a thermoelectric device, and it is an irreversible process where heat is generated due to electrical current flow in a conductor.

Thermoelectrical systems have low maintenance due to the lack of moving parts, are highly reliable and more environmentally friendly [7]; however, the energy conversion efficiency is low, usually below 10% [8], which hinders its use on some applications. The efficiency can be increased using materials with better properties, with theoretical efficiencies as high as 25% [9]. In line with the simulations, the interest in the topic was renewed with the advent of new materials, such as semiconductors [10].

One of the most important parameter of a thermoelectric device is the thermoelectric dimensionless figure of merit (ZT), defined as $ZT = S^2\sigma T/k$, where S is the pair Seebeck coefficient (V/K), σ is the electrical conductivity ($1/(\Omega m)$), T is the temperature (K), and k is the thermal conductivity (W/(m K)). Typical materials used in the thermocouples are metals and semiconductors [11], with Bi_2Te_3 and Sb_2Te_3 being the most common materials [10]. Doping allows materials with high thermal conductivity to be adequate for thermoelectric applications, such as Nb-doped TiO_2 [12] or Si-doped graphene [13].

The association of several thermoelectric pairs in series is called a thermoelectric module, which can easily exceed more than one hundred elements connected in series. A typical thermoelectric module can be used for both refrigeration and thermoelectric generation [11, 14, 15].

Several applications use the thermoelectric effect, including cooling in systems with low thermal loads (drinking fountains, mini-wine cellars), and thermoelectric generation in space applications [16]. Xu et al. [17] proposed a man-portable cooling garment to relieve thermal stress on workers in hot environment. Cold water circulated the garment which was then cooled by a thermoelectric device, and afterward returning to the garment, closing the loop. The thermoelectric device had 197 couples of N-P semi-conductors, using 100 W electrical power to produce 340.4 W of cooling power with a temperature difference of 75 °C.

Ji et al. [18] proposed an integrated cooling–heating system for sterilization of air to inactivate SARS-CoV-2 virus. They simulated modules with Seebeck coefficient of $S = 2.06 \cdot 10^{-4}$ V/K, $\sigma = 100k\Omega/m$ and $k = 1.5W/(m K)$, obtaining a ZT of 1.7 and a cooling COP of 5.4. Di Capua and Jahn [19] proposed a thermoelectric self-cooling system to refrigerate electronic devices. Zhao et al. [20] simulated a sky cooling-assisted thermoelectric cooling system

for building applications, using modules with $ZT = 0.80$, obtaining a yearly average COP of 1.87. Pourkiaei et al. [21] provide a revision comprising cooling and power generation applications.

Considering the context of new applications with thermoelectric systems, this work proposes a concept of a triple thermoelectric system, involving integrated cooling, heating and thermoelectric generation. No work from literature was identified with a system able to cool, heat water and generate electrical energy by thermoelectric phenomena in an single integrated device. Thus the objective of this work is to evaluate the performance of the proposed system through numerical simulation and experimental tests. Two configurations of the system were investigated, (i) water thermoelectric cooling/heating system and (ii) cold/hot water thermoelectric generation system. This concept is intended to be applied for water cooling/heating or for electricity generation in isolated communities and in non-urban regions. Additionally, it was used a model for thermoelectric modules that is based only on manufacturer data commonly available on datasheets. The experimental results of this work are valuable information that can be used in new modeling studies and specification of similar systems.

2 System modeling

The concept of the proposed system is illustrated in Fig. 1. It consists of two water reservoirs, one for hot water and one for cold water, which are thermally interconnected by two parallel thermoelectric modules installed between two heat sinks. Heat sinks are in contact with reservoir's water, exchanging heat by natural or forced convection, depending on the application. Each reservoir can hold a volume of up to 2 L of water. This system can operate in two modes: (i) water cooler/heater, (ii) thermoelectric generator. In cooling/

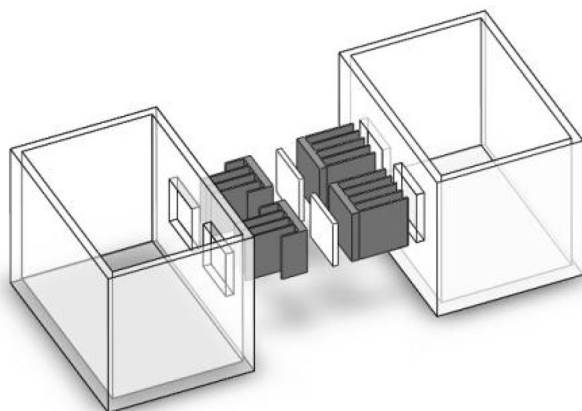


Fig. 1 3D design of the proposed system

heating mode the two thermoelectric modules operate with parallel electrical connection; in generator mode, the modules operate with series electrical connection. Commercial thermoelectric modules type TEC12706 [22], $40 \times 40 \text{ mm}^2$ in size 127 couples of BiSn are used. In cooling/heating mode, electrical current is supplied to the module from an external direct current source and in generation mode the thermoelectric module supplies electrical power to an external electrical load.

2.1 Model for cooling/heating system

Figure 2 shows the three subsystems involved in modeling the proposed system when operated in cooling/heating mode. In this operational condition, the system provides chilled and heated water in the cold and hot reservoirs, respectively. The model predicts the evolution of water temperatures in the two reservoirs, the heat exchange between them, the heat exchange with the environment, the cooling/heating system COP, and the voltage and electrical current in the modules.

Figure 3 shows a simplified thermal resistance model used in thermal modeling. For each reservoir, the heat transfer with the environment (radiation, convection and conduction) is modeled by $R_{env,C}$ and $R_{env,H}$, while the internal heat transfer by convection and conduction in heat sinks and modules is modeled using $R_{thm,C}$ and $R_{thm,H}$. The respective heat transfer rates to or from cold and hot reservoirs are Q_C (cold side) and Q_H (hot side), respectively. The energy conservation equations are written for each reservoir and are given by Eqs. 1 and 2. The coupling of the equation system is performed through energies balances by Eqs. 3 and 4.

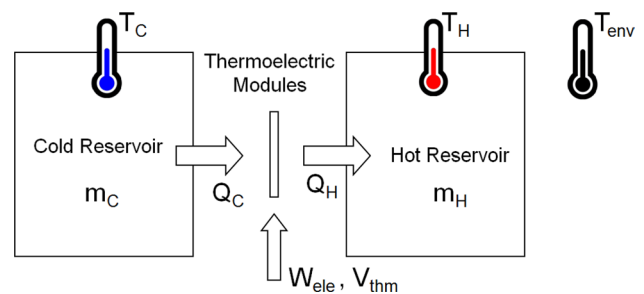


Fig. 2 Subsystems involved in system modeling

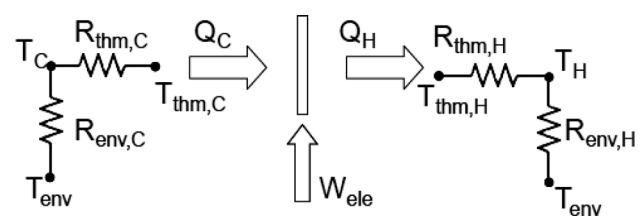


Fig. 3 Simplified thermal model

$$m_c c_{p,C} \frac{dT_C}{dt} = Q_{in} - Q_{out} = \frac{T_{env} - T_c}{R_{env,C}} - Q_C \tag{1}$$

$$m_H c_{p,H} \frac{dT_H}{dt} = Q_{in} - Q_{out} = Q_H - \frac{T_H - T_{env}}{R_{env,H}} \tag{2}$$

$$Q_H = \frac{T_H - T_{thm,H}}{R_{thm,H}} \tag{3}$$

$$Q_C = \frac{T_C - T_{thm,C}}{R_{thm,C}} \tag{4}$$

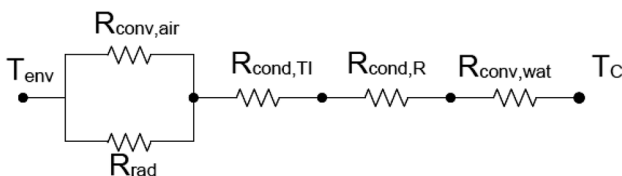
$$R_{env,C} = \frac{R_{rad} R_{conv,air}}{(R_{rad} + R_{conv,air})} + R_{cond,TI} + R_{cond,R} + R_{conv,wat} \tag{5}$$

$$R_{thm,C} = R_{HS} + R_{CR} + R_{cer} \tag{6}$$

In Eqs. 1–4 the sub-indexes *C* and *H* stand for the cold and hot reservoirs, respectively. m_C and m_H are the equivalent system masses of each reservoir, since in the model the sub-element masses (water, heat sinks, thermal insulation and modules) are grouped under single terms. The equivalent specific heat is indicated by c_p . T_C and T_H represent the water temperature in cold and hot sides, T_{env} is the environment temperature, and T_{thm} stands for junction temperature of thermoelectric module. $R_{env,C}$ and $R_{env,H}$ represent the thermal resistances between the external environment and water for each reservoir, while $R_{thm,C}$ and $R_{thm,H}$ are the thermal resistances between the water and cold or hot thermoelectric module junctions, respectively.

Figure 4a shows a more detailed description of the thermal resistance between the environment and the water of the cold reservoir ($R_{env,C}$). This thermal resistance is represented by the effective thermal circuit modeled by Eq. 5. The thermal circuit considers the following heat transfer

(a) $R_{env,C}$



(b) $R_{thm,C}$

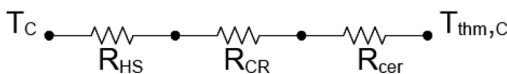


Fig. 4 Detailed calculation of cold side resistance: **a** $R_{env,C}$, **b** $R_{thm,C}$

mechanics and thermal resistances: external radiation (R_{rad}) and natural air convection ($R_{conv,air}$), conduction heat transfer through both the thermal insulation ($R_{cond,TI}$) and the reservoir walls ($R_{cond,R}$) and the internal water natural convection ($R_{conv,wat}$). Both air and water natural convection processes have been calculated with the Churchill and Chu [23] correlations for laminar and turbulent-free convection from a vertical plate. The equivalent circuit of thermal resistance between cold water and thermoelectric junction ($R_{thm,C}$) is shown in Fig. 4b and is modeled by Eq. 6. This circuit includes the heat sink convection/conduction (R_{HS}), the conductive contact resistance R_{CR} and thermal resistance of the ceramic electric insulation layer (R_{cer}). Analogous modeling approach has been applied to the hot reservoir and for the modeling of the thermoelectric generation system, shown in Sect. 2.2. For the thermoelectric modules in heating/cooling mode, the energy conservation is given by Eq. (7).

$$Q_H = Q_C + W_{ele} \tag{7}$$

The equations that determine the thermoelectric coupling of the module based on maximum parameters are given by Eqs. (8) and (9) [24].

$$Q_C = 2Q_{max} \left(\frac{i}{i_{max}} \right) - \left(\frac{i}{i_{max}} \right)^2 - \left(\frac{\Delta T_{thm}}{\Delta T_{thm,max}} \right) \tag{8}$$

$$\left(\frac{V_{thm}}{V_{max}} \right) = \frac{\left(\frac{\Delta T_{thm}}{\Delta T_{thm,max}} \right) \frac{ZT_c}{2} + \left(\frac{i}{i_{max}} \right)}{\frac{ZT_c}{2} + 1} \tag{9}$$

where i is the electrical current, V_{thm} is the electrical voltage in the module, ZT_c is dimensionless figure of merit of the module at cold junction temperature reference. T_c in Kelvin, and ΔT_{thm} is the temperature difference between the junction within the module. The dimensionless figure of merit can be estimated by Eq. 10 [25]. An average T_c temperature of 288 K and the value of $ZT_c = 0.76$ were used for simulation purposes in the cooling/heating system.

$$ZT = \frac{2\Delta T_{max} T_c}{(T_{href} - \Delta T_{max})^2} \tag{10}$$

The electrical power consumed by each module is given by:

$$W_{ele} = V_{thm} i \tag{11}$$

The definitions of cooling and heating efficiencies are given by Eqs. 12 and 13, respectively.

$$COP_C = \frac{Q_C}{W_{ele}} \tag{12}$$

$$COP_H = \frac{Q_H}{W_{ele}} \tag{13}$$

Table 1 shows the thermoelectric module data used for the model solution and input voltage used in the experiments for the cooling/heating system. Geometry and maximum performance specifications were obtained from the manufacturer datasheet [22].

2.2 Model for thermoelectric generation system

The thermoelectric model for the system operating in generator mode differs basically by reversing the directions of the heat exchanged in the thermoelectric module and the direction of the electrical energy that now is supplied by the thermoelectric module as an electrical generator. In this mode, heated water is placed in the hot reservoir and cold water in the cold reservoir. The heat exchanged through the modules will allow the thermoelectric generation, Fig. 5. The energy balance in the reservoirs and coupling equations is given, respectively, by Eqs. 14–18.

$$m_c c_{pC} \frac{dT_C}{dt} = Q_{in} - Q_{out} = \frac{T_{env} - T_c}{R_{env,C}} - Q_C \tag{14}$$

$$m_H c_{pH} \frac{dT_H}{dt} = Q_{in} - Q_{out} = -Q_H - \frac{T_H - T_{env}}{R_{env,H}} \tag{15}$$

$$Q_H = Q_C + W_{ele} \tag{16}$$

$$Q_H = \frac{T_H - T_{thm,H}}{R_{thm,H}} \tag{17}$$

$$Q_C = \frac{T_C - T_{thm,C}}{R_{thm,C}} \tag{18}$$

Taking into account that the efficiency of thermoelectric generation is low, the electric power is negligible compared against the rate of heat rejected (Q_C). Thus, the approximation expressed by Eq. 19 was assumed.

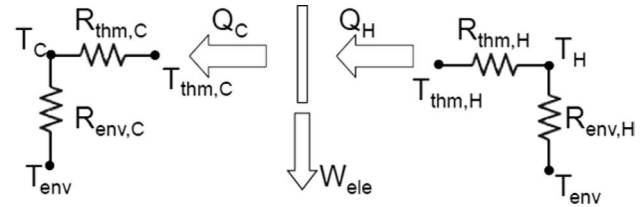


Fig. 5 Simplified thermal model of the power generator system

$$W_{ele} \ll Q_C \Rightarrow Q_H \approx Q_C \tag{19}$$

The heat transfer through the module is given by Eq. 20 where $R_{th,m}$ is thermal resistance of the thermoelectric module.

$$Q_H = Q_C = \frac{T_{thm,H} - T_{thm,C}}{R_{th,m}} \tag{20}$$

Equation 21 gives the generated electrical current,

$$i = \frac{S_m}{R_L + R_m} (T_{thm,H} - T_{thm,C}) \tag{21}$$

where S_m is the Seebeck coefficient of the module, R_m is the electrical resistance of the module, and R_L is the electrical resistance of the load to which the generator will be connected.

The module thermal resistance, $R_{th,m}$, Seebeck coefficient, S_m , and electrical resistance, R_m , are obtained from the thermoelectric module maximum parameters, shown in Table 2, with the aid of Eqs. 22 to 26 [25].

$$Z_m = \frac{2\Delta T_{max}}{(T_{h,ref} - \Delta T_{max})^2} \tag{22}$$

$$K_m = \frac{1}{2} \frac{T_{h,ref} - \Delta T_{max}}{T_{h,ref} \Delta T_{max}} (Vi)_{max} \tag{23}$$

$$R_m = \frac{(T_{h,ref} - \Delta T_{max})}{T_{h,ref}} \left(\frac{V}{i} \right)_{max} \tag{24}$$

$$S_m = (Z_m R_m K_m)^{0.5} \tag{25}$$

Table 1 Data for the thermoelectric module on cooling/heating mode [22]. $T_H = 50^\circ\text{C}$

Parameter	Value
Q_{max}	67 W
V_{max}	17.2 V
i_{max}	6.1 A
ΔT_{max}	79 K
$A_{peltier}$	40 × 40 mm ²

Table 2 Main parameter values for the thermoelectric module

Parameter	Value
S_m (mV/K)	53.3
Z_m (K ⁻¹)	0.002654
ZT_m (-)	0.84
K_m (W/K)	0.50
R_m (Ω)	2.1

$$R_{th,m} = 1/K_m \quad (26)$$

$$(ZT)_m = \frac{Z_m(T_{c,m} + T_{h,m})}{2} \quad (27)$$

where Z_m is the module figure of merit, K_m is the module thermal conductance, and ZT_m is the module dimensionless figure of merit. The hot side temperature reference used for the above parameters reference was $T_{H,ref} = 323 \text{ K} = 50 \text{ }^\circ\text{C}$.

The first law thermal efficiency for thermoelectric generator is given by

$$\eta = \frac{W_{ele}}{Q_H} \quad (28)$$

where the power generated at the load is

$$W_{ele} = i^2 R_L \quad (29)$$

3 Experimental setup

Figure 6 shows a photograph of the final built prototype used to validate the system's model. The experiments were performed with an approximate volume of 1.8 L in each reservoir, which has the following internal dimensions: $160 \times 120 \times 110 \text{ mm}^3$. A 20-mm-thick Styrofoam has been used on all reservoir surfaces for external wall insulation (including the lid) to minimize losses to the environment. A thermal conductivity value of 33 mW/m.K for the Styrofoam was used in the simulations.

During the experiment the measured variables were cold water and hot water temperatures, room temperature and

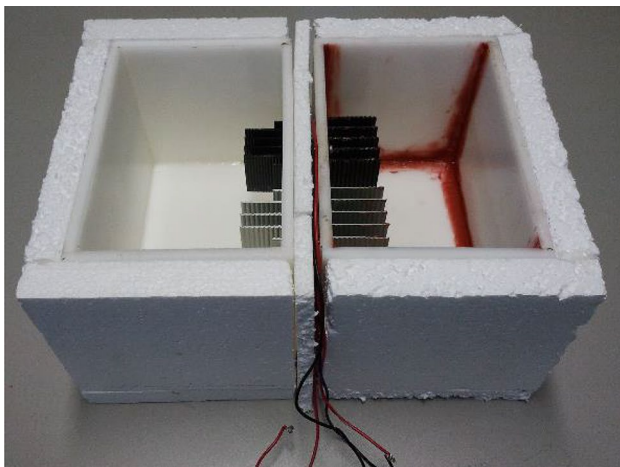


Fig. 6 Prototype of the proposed system

electrical tension on the output of the thermoelectric modules, as indicated in Fig. 2. Temperatures were measured by using three type T thermocouples. The hot water and cold water thermocouples were placed in the middle of their respective reservoirs. Before each measurement a plastic spoon was used for mixing the water, avoiding temperature stratification errors. The experimental data were registered at time intervals between 1 and 10 min depending on the experiment. The values were manually recorded at regular time intervals. All the instruments were placed side by side, and a cell phone was used to take photographs of the instruments for the register of the experimental values at desired instant. Each photograph had the time recorded with 1 s resolution. The experimental uncertainties are: temperatures ($0.5 \text{ }^\circ\text{C}$) using a calibrated type T thermocouples reader, voltage (1%) and electrical current (2%) using a Minipa Multimeter, time ($< 1 \text{ s}$) from the cell phone, dimensions (1 mm) and mass (10 g), using a digital scale. Water and air properties were obtained through the Engineering Equation Solver (EES)[®] [26]. For all experiments an insulation lid of 20 mm was placed on top of the system, Fig. 6, to reduce heat transfer to external environment. The external air temperature during the experiments was $25 \text{ }^\circ\text{C}$, and this value was used for the simulations.

4 Results

This section presents the results obtained with the simulation model and the experimental measurements in the prototype, considering operations in both the cooling/heating mode and the thermoelectric generation mode. The simulation results and the experimental data are compared.

4.1 Heating/cooling water

The first test is shown in Fig. 7 for heating/cooling mode considering that water at the initial temperature of $25 \text{ }^\circ\text{C}$ was placed in each reservoir. The thermoelectric modules were connected to an 11.7 V DC power supply in order to cool one side and heat the other. The reservoirs were closed with the insulation and the evolution of temperatures over time verified.

Figure 7 shows a good agreement between simulation results and experimental data for both hot and cold water. In this experiment the hot water reached $70 \text{ }^\circ\text{C}$, while water in the cold reservoir was cooled to around $17 \text{ }^\circ\text{C}$.

It can be observed that the water in the cold reservoir would start to heat up due to the excess temperature in the heated reservoir for time above 50 min, a fact predicted by the simulation model. Analyzing the COP, it can be seen that heating COP was above 1.4, showing that the system is more efficient for heating than the use of pure electrical resistance. The cooling COP reaches a value near 0.4.

Fig. 7 Evolution of water temperature in reservoirs and COP in heating mode

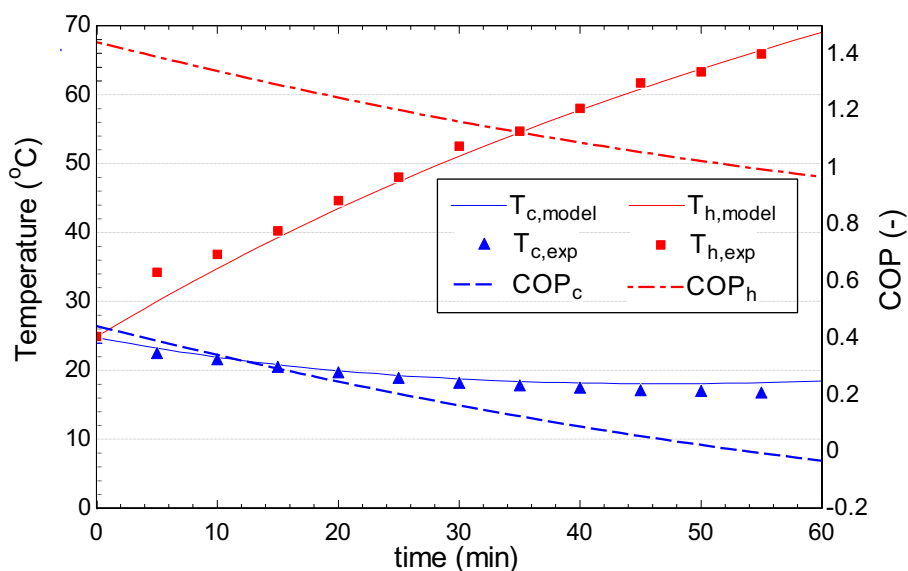


Figure 8a shows the electrical power consumed by one thermoelectric module and the heat rate exchanged in the hot and cold reservoirs calculated by the model. When time approaches 50 min the cooling capacity, Q_c , becomes negative, indicating that the cold reservoir would start a heating processes. This process can be easier understood with the aid of Fig. 8b, which shows the thermoelectric module cold and hot junction temperatures ($T_{thm,C}$, $T_{thm,H}$) against the water temperature in the cold and hot reservoirs (T_C , T_H). When time approaches 50 min, it can be noted that the cold junction of the thermoelectric module is warmer than the water in the cold reservoirs, explaining why the heating process starts at this moment.

4.2 Cooling water at low temperature

The second test was also in the cooling/heating mode but with the solo objective of cooling water in the cold reservoir. To achieve this goal more efficiently, the water in the hot reservoir was periodically and partially renewed in order to keep it at near a constant temperature of approximately 35 °C. Figure 9 shows the model and experimental results for this experiment.

In this experiment, the cold side water quickly reached 0 °C; the cooling COP was between 0.2 and 0.4 during the experiment and the heating COP between 1.2 and 1.4. The hot water temperature used on the model was set to a fixed value of 35 °C. The variation of experimental hot water temperature around 35 °C is due the manual control of the hot water temperature by periodic renewal portion of it with new cooler water.

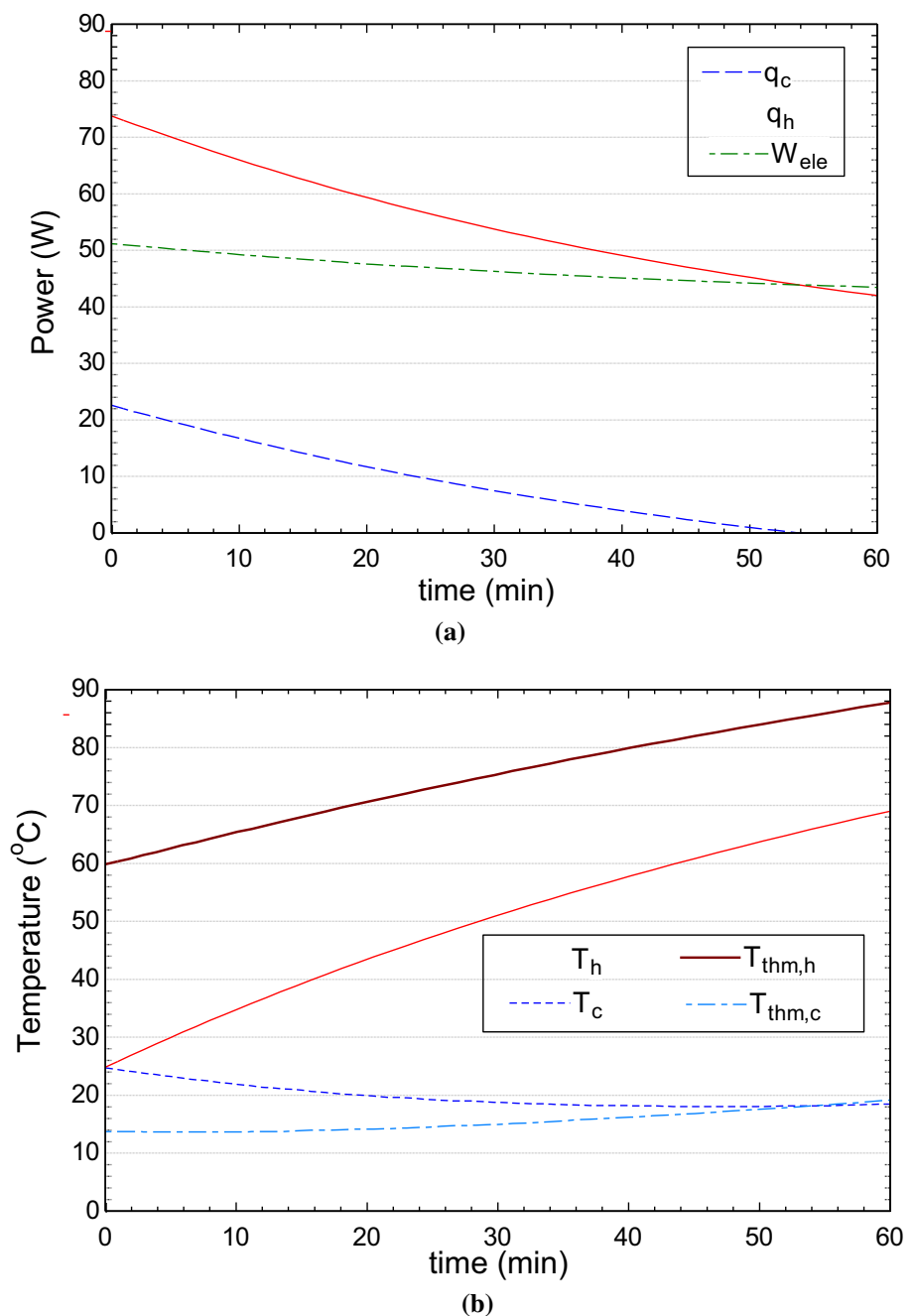
4.3 Thermoelectric generation (thermal battery)

The third test performed was in thermoelectric generation mode. In this one, water preheated to near 80 °C with an electrical heater was added in the hot reservoir and chilled water near 10 °C with the use of a refrigerator was added in the cold reservoir. These temperatures were chosen because it could be easily reproduced in the experiments and a difference of 70 °C can be easily obtained in most of climates by boiling water, for example. The heat transfer between the two reservoirs through the thermoelectric modules allowed the generation of electricity that was measured and compared with the simulation model described in Sect. 2.2. The results are presented in Fig. 10. It is observed again a good agreement between the simulation and experimental results, considering the variation of cold and hot water temperatures, and the generated electrical voltage over time. In the case of electrical voltage, the load resistance used in the results presented in Fig. 10 was $R_L = 84 \Omega$. The system had an initial voltage of 4.7 V and could run for approximately 53 min before reaching a 2-V voltage level.

For an electrical load resistance of $R_L = 4 \Omega$ the maximum generation thermal efficiency was 3%. In a Carnot cycle, between the same reservoirs, the maximum value would be 19%. In the condition of $R_L = 4 \Omega$, the generation power exceeded 1.75 W. This power level is sufficient for charging mobile phones, running flashlights and even small electric motors. If the initial values of temperature difference can be maintained, this power level can be kept continuously.

Table 2 shows the main parameter values for the thermoelectric module in generator mode. These values were calculated using Eqs. 22 to 27 with the input data of Table 1.

Fig. 8 Model transient results, **a** hot and cold side heat rates and the electrical power in heating mode, and **b** thermoelectric module temperatures ($T_{\text{thm,H}}$ and $T_{\text{thm,C}}$) versus water temperature in reservoirs (T_{H} and T_{C})



As a final application for the proposed thermoelectric generation system, the developed model was used to determine the size of a reservoir needed to run as a thermal battery for at least 12 h (720 min) continuously using exactly the same two thermoelectric modules and with higher initial temperatures of the hot and cold reservoir of 95 °C and 25 °C, respectively. The simulation shown in Fig. 11 indicated that reservoirs with 25-L capacity of water are needed. For a load resistance of 4 Ω (load similar to a cell phone) the system can supply energy down to 1 V level during more than 800 min, which is equivalent to more than

6 alkaline AA battery. The hot reservoir could be heated using any available heat source, as dry straw or wood, solar energy, making the system practical to be used as an alternated generation system for isolate communities. This type of thermal battery has long endurance, low price, can use multiple energy sources and could work for years without need of replacing parts. In industrial scale this system could be produced below US\$ 10.00 cost per unit, indicating that it can be a helpful, low cost and reliable solution for providing basic energy needs around the world.

Fig. 9 Evolution of water temperature in reservoirs and COP in cooling mode

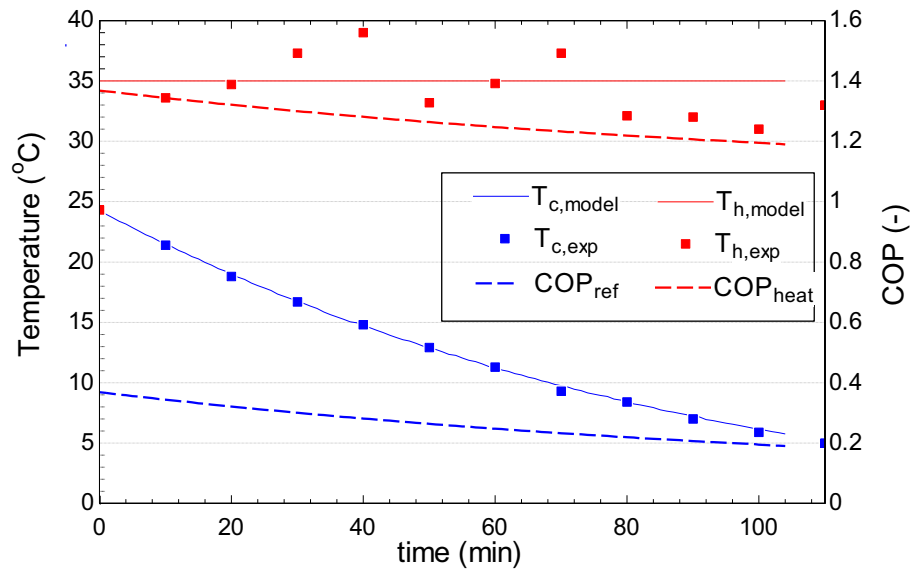
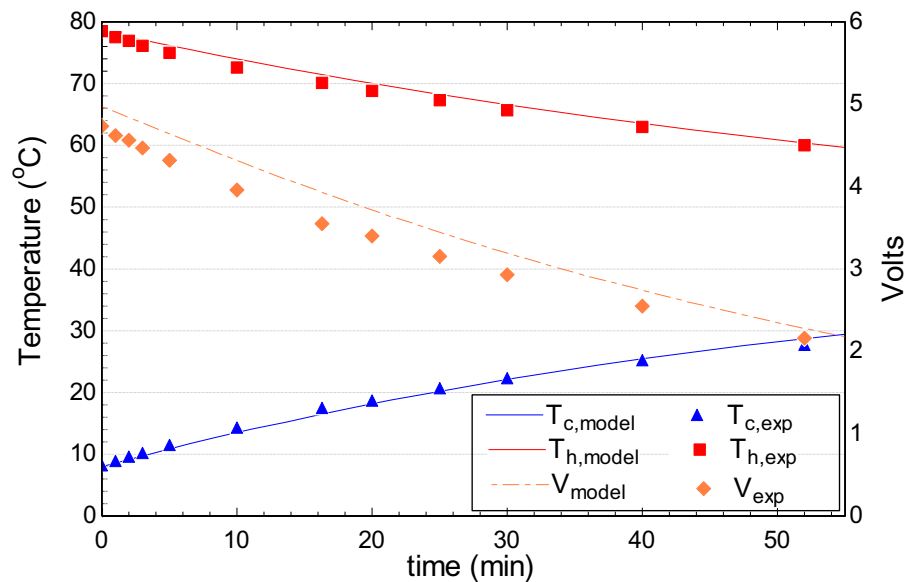


Fig. 10 Evolution of reservoirs water temperatures and voltage generated in thermoelectric generator mode. $R_L = 84 \Omega$

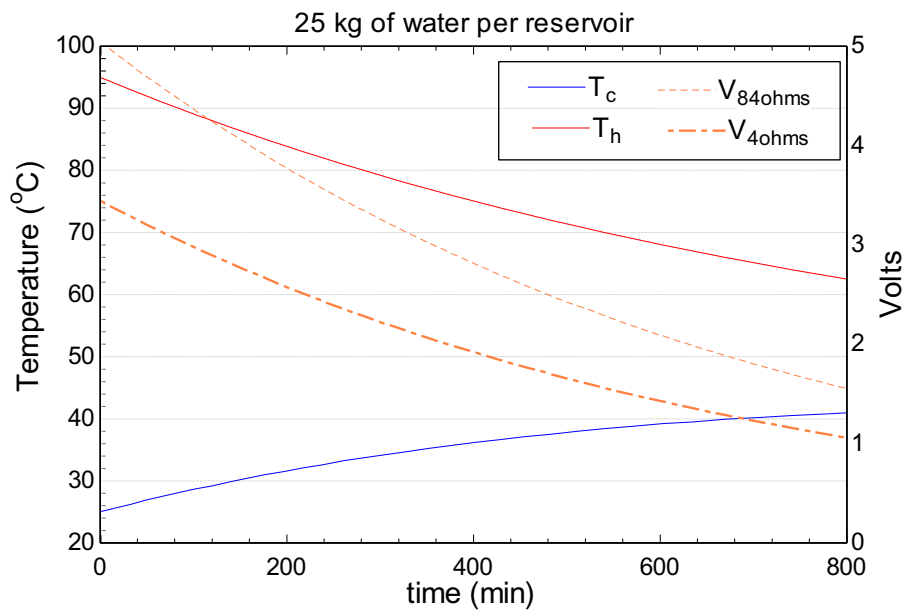


5 Conclusions

A new conceptual design of an integrated system for cooling, heating and thermoelectric generation using water was presented. No previous work from the literature was identified with a system able to cool, heat water and generate electrical energy by thermoelectric phenomena in an single integrated device. The model uses maximum performance parameters available in commercial thermoelectric datasheets to obtain all other relevant thermoelectric variables. The agreement between the developed model and experiment data was close to 95% (average error of 1.7% in temperatures and 8% in electric voltage), and the proposed systems were able to cool water near zero degree, heat it

near the water boiling point and generate more than 1.5 W of electrical power when operated in thermoelectric generator mode. The system can function as a heated water-powered thermoelectric battery and can be equivalent to a 1-Wh capacity AA-type battery operating from 1.8 L heated water at 80 °C and 1.8 L chilled water at 10 °C. The simulations also showed that a reservoir of 25 L of water at 95 °C could be used to supply peak electrical power of 2.3 W and mean power of 1 W for 12 h, energy equivalent to 6 AA alkaline batteries. This system is intended to be applied for sustainable cooling, heating and electricity generation in isolated communities and in outdoor activities in non-urban regions. It can be a helpful, low-cost and reliable solution for providing basic energy needs around the world.

Fig. 11 Evolution of reservoirs water temperatures and voltage generated in thermoelectric generator mode for reservoirs with 25 L capacity



Acknowledgements This work was carried out with the support of the Coordination of Superior Level Staff Improvement—Brazil (CAPES)—Financing Code 001 and the Graduate Program in Mechanical Engineering from EESC-USP.

Declarations

Conflict of interest We declare that author Luben Cabezas-Gómez acts as Associate Editor for this journal.

References

- United Nations (1992) United Nations framework convention on climate change. Rio de Janeiro, Brazil
- United Nations Environment Program, The Kigali Amendment (2016): The amendment to the Montreal protocol agreed by the twenty-eighth meeting of the parties. Kigali, Ruanda, 2016.
- Tibiriçá CB, Ribatski G (2013) Flow boiling in micro-scale channels – synthesized literature review. *Int J Refrig* 36(2):301–324. <https://doi.org/10.1016/j.ijrefrig.2012.11.019>
- Mota-Babiloni A (2015) Analysis on EU Regulation No 517/2014 of new HFC/HFO mixtures as alternatives of high GWP refrigerants in refrigeration and HVAC systems. *Int J Refrig* 52:21–31
- David TM, Buccieri GP, Rizol PMSR (2021) Photovoltaic systems in residences: a concept of efficiency energy consumption and sustainability in Brazilian culture. *J Clean Prod* 298:126836
- Pali BS, Vadhera S (2021) A novel approach for hydropower generation using photovoltaic electricity as driving energy. *Appl Energy* 302:117513. <https://doi.org/10.1016/j.apenergy.2021.117513>
- Sajid M (2017) An overview of cooling of thermoelectric devices. *Renew Sustain Energy Rev* 78:15–22
- Liu W, Jie Q, Kim HS, Ren Z (2015) Current progress and future challenges in thermoelectric power generation: From material to devices. *Acta Mater* 87:357–376
- Ryu B, Chung J, Park SD (2021) Thermoelectric degrees of freedom determining thermoelectric efficiency. *iScience* 24(9):102934. <https://doi.org/10.1016/j.isci.2021.102934>
- Snyder GJ, Toberer ES (2008) Complex thermoelectric materials. *Nat Mater* 7:105–114
- Zhao D, Tan G (2014) A review of thermoelectric cooling: Materials, modeling and applications. *Appl Therm Eng* 66:15–24
- Ribeiro JM et al (2021) Transparent niobium-doped titanium dioxide thin films with high Seebeck coefficient for thermoelectric applications. *Surf Coat Technol* 425:127724
- Lee W, Lim G, Ko SH (2021) Significant thermoelectric conversion efficiency enhancement of single layer grapheme with substitutional silicon dopants. *Nano Energy* 87:106188
- Riffat SB, Ma X (2003) Thermoelectrics: a review of present and potential applications. *Appl Therm Eng* 23:913–935
- Enescu D, Virjoghe EO (2014) A review on thermoelectric cooling parameters and performance. *Renew Sustain Energy Rev* 38:903–916
- Bell LE (2008) Cooling, heating, generating power, and recovering waste heat with thermoelectric systems. *Science* 321:1457–1461
- Xu Y et al (2022) Man-portable cooling garment with cold liquid circulation based on thermoelectric refrigeration. *Appl Therm Eng* 200:117730
- Ji R et al (2021) An integrated thermoelectric heating-cooling system for air sterilization. *Mater Today Phys* 19:100430
- Di Capua MH, Jahn W (2020) Performance assessment of thermoelectric self-cooling systems for electronic devices. *Appl Therm Eng* 193:117020
- Zhao D et al (2020) Radiative sky cooling-assisted thermoelectric cooling system for building applications. *Energy* 190:1163222
- Pourkiaei SM et al (2019) Thermoelectric cooler and thermoelectric generator devices: a review of present and potential applications, modeling and materials. *Energy* 186:115849
- Thermonamic Module. Specification of Thermoelectric Module TEC1–12706. www.thermonamic.com.cn
- Churchill SW, Chu HHS (1975) Correlating equations for laminar and turbulent free convection from a vertical plate. *Int J Heat Mass Transf* 18:1323–1329
- Lee H-S (2010) Thermal design: heat sinks, thermoelectrics, heat pipes, compact heat exchangers, and solar cells. Wiley & Sons, New Jersey

25. Luo Z (2008) A simple method to estimate the physical characteristics of a thermoelectric cooler from vendor datasheets. *Electron Cool* 14(3):22–27
26. EES, F-chart, <http://www.fchart.com/ees>

Publisher's Note Springer Nature remains neutral with regard to jurisdictional claims in published maps and institutional affiliations.

Springer Nature or its licensor holds exclusive rights to this article under a publishing agreement with the author(s) or other rightsholder(s); author self-archiving of the accepted manuscript version of this article is solely governed by the terms of such publishing agreement and applicable law.